



ELSEVIER

Available online at www.sciencedirect.com ScienceDirect

Proceedings of the Combustion Institute 31 (2007) 149–157

**Proceedings
of the
Combustion
Institute**

www.elsevier.com/locate/proci

Rate constants for the H abstraction from alkanes (R–H) by R'O₂ radicals: A systematic study on the impact of R and R'

Hans-Heinrich Carstensen^{a,*}, Anthony M. Dean^a, Olaf Deutschmann^b^aChemical Engineering Department, Colorado School of Mines, Golden, CO 80401, USA^bInstitute for Technical Chemistry and Polymer Chemistry, University Karlsruhe (TH), Kaiserstr. 12, 76131 Karlsruhe, Germany

Abstract

A possible source of chain-branching in low temperature combustion is thermal decomposition of alkyl hydroperoxides (R'OOH). One way these species can be produced is via H atom abstraction reactions from alkanes (RH) by alkylperoxy radicals R'O₂. An earlier study focussing on the abstraction from ethane by HO₂, CH₃O₂ and C₂H₅O₂ revealed that these reactions have a noticeable impact on calculated ignition times of ethane/O₂ mixtures. Another outcome was that the abstraction rate constants for CH₃O₂ and C₂H₅O₂ are virtually identical but smaller than that for HO₂. The associated activation energies followed an Evans–Polanyi relationship while a common A-factor could be used to describe the kinetics of all three reactions within a factor of about 2–3. In this current study, we extend the investigation by (1) considering a set of alkanes (RH = CH₄, C₂H₆, C₃H₈, C₄H₁₀) and (2) by including additional peroxy species (R'O₂ with R' = H, CH₃, C₂H₅, C₃H₇, C₄H₉, HC=O, and CH₃C=O). We present rate constants for a total of 32 reactions and analyze the data with respect to systematic trends in the reactivity. The results reveal that the rate constants decrease in the order acylperoxy > HO₂ > alkylperoxy. The reactivity of different C–H bonds follows the bond strengths. Overall the heat of reaction is found to be the dominant but not the only rate constant controlling parameter. The accuracy of the calculations and implications of the results are discussed.

© 2006 The Combustion Institute. Published by Elsevier Inc. All rights reserved.

Keywords: Peroxy radical chemistry; Hydrogen abstraction; Ab initio calculations; Transition state theory; Low temperature oxidation

1. Introduction

The oxidation of hydrocarbons at low to intermediate temperatures is a complex process, as

phenomena such as the negative temperature coefficient (NTC) or the existence of two-step ignition processes illustrate. According to Walker and Morley [1] the chemistry is mainly dominated by the formation and reactions of alkylperoxy radicals, R'O₂, which can either promote or inhibit ignition. More specifically, rearrangement of R'O₂ to the hydroperoxy radical, R'OOH, followed by subsequent reaction with O₂ is believed

* Corresponding author. Fax: +1 303 273 3730.

E-mail address: hcarsten@mines.edu (H.-H. Carstensen).

to be the most important source for chain-branching since this sequence produces two or more $\cdot\text{OH}$ radicals [2]. On the other hand, $\text{R}'\text{O}_2$ radicals decompose with increasing temperature to $\text{R}' + \text{O}_2$ hence reducing the amount of $\text{R}'\text{O}_2$ available for this chain-branching route. Consequently, the ignition time increases and we observe NTC behavior, meaning the existence of a temperature region in which the overall reactivity declines with increasing temperature. A further complication in this scheme arises from the production of alkene + HO_2 . It is long known that these products can be formed from $\text{R}'\text{OOH}$ via simple bond fission, but recently a second low-energy path originating directly from $\text{R}'\text{O}_2$, the concerted elimination channel, has firmly be established [3–7]. Assuming that HO_2 mainly reacts to form H_2O_2 , which is rather stable at low temperatures, one would expect that the alkene channel inhibits the ignition process. This leads to the question whether enough chain-branching can be produced from unimolecular $\text{R}'\text{O}_2$ reactions alone.

Of course, $\text{R}'\text{O}_2$ radicals can also participate in bimolecular reactions and these routes have been considered by Walker and Morley as well. Besides the recombination of alkyl peroxy radicals and their reaction with HO_2 , abstraction reactions from hydrocarbons are of special interest because they lead to the formation of alkyl hydroperoxides, $\text{R}'\text{OOH}$, which have weak O–O bonds. For example the O–O bond dissociation energies for

$\text{CH}_3\text{O}-\text{OH}$ and $\text{C}_2\text{H}_5\text{O}-\text{OH}$ are about 44 kcal/mol, which may be compared to the value of 50 kcal/mol found for H_2O_2 [8]. Noticing that H_2O_2 decomposition is the major source of chain-branching at temperatures *above* the NTC region, the intriguing possibility arises that the increased reactivity observed around 600 K might be related to the fission of $\text{R}'\text{OOH}$ bonds. Thus, H abstraction by $\text{R}'\text{O}_2$ radicals followed by the thermal decomposition of $\text{R}'\text{OOH}$ might provide additional chain-branching in the low temperature oxidation of hydrocarbons to offset the loss due to the concerted elimination channel. In any case, oxidation models would be incomplete if these reactions were missing.

A prerequisite to incorporating $\text{R}'\text{O}_2$ abstraction reactions into oxidation models is the availability of reliable rate parameters. Kinetic measurements are very difficult because of the dominating influence of $\text{R}'\text{O}_2$ recombination and other side reactions (e.g., with HO_2) and to the best of our knowledge no experimental rate constants have been reported. A similar situation exists for abstraction reactions by HO_2 , though Walker and coworkers [9–14] have been able to assign rate constants for several alkanes from the analysis of complex reaction systems. An alternative source of kinetic parameters is rate theory, but surprisingly little work has been done on these systems. Tsang et al. [15–17] report rate expressions for abstraction reactions of HO_2 and CH_3O_2 with small alkanes,

Table 1
Rate constants (in cm^3/mols) of the entire set of $\text{R}'\text{O}_2 + \text{R}-\text{H}$ reactions at 600 and 800 K, respectively

R–H	CH_4		C_2H_6		C_3H_8		C_4H_{10}	
$\text{R}'\text{O}_2$	600 K	800 K	600 K	800 K	600 K	800 K	600 K	800 K
HO_2	3.25E4	6.09E6	1.12E6	8.11E7	9.04E5	6.25E7 ^a	1.09E6	7.18E7 ^c
					8.01E6	2.78E8 ^b	1.21E7	4.14E8 ^d
							1.10E6	7.45E7 ^e
							4.36E7	8.40E8 ^f
CH_3O_2	5.92E3	1.51E6	1.95E5	1.88E7	1.02E5	1.03E7 ^a	1.98E5	1.98E7 ^c
							3.30E6	1.52E8 ^d
					1.74E6	8.26E7 ^b	1.17E5	1.20E7 ^e
							1.04E7	2.65E8 ^f
$\text{C}_2\text{H}_5\text{O}_2$	3.74E3	9.60E5	1.69E5	1.67E7	6.02E4	6.22E6 ^a	—	—
					8.63E5	4.44E7 ^b	—	—
$n\text{-C}_3\text{H}_7\text{O}_2$	1.02E3	2.85E5	5.75E4	6.40E6	—	—	—	—
$i\text{-C}_3\text{H}_7\text{O}_2$	2.08E3	6.11E5	7.96E4	9.08E6	—	—	—	—
$n\text{-C}_4\text{H}_9\text{O}_2$	1.75E3	5.01E5	—	—	—	—	—	—
$t\text{-C}_4\text{H}_9\text{O}_2$	1.16E3	3.58E5	—	—	—	—	—	—
HC(O)O_2	4.72E6	2.79E8	5.21E7	1.09E9	6.12E7	1.43E9 ^a	—	—
					1.16E9	1.37E10 ^b	—	—
$\text{CH}_3\text{C(O)O}_2$	4.74E6	2.62E8	3.93E7	7.55E8	—	—	—	—

See text for details.

^a $n\text{-C}_3\text{H}_7$ channel.

^b $i\text{-C}_3\text{H}_7$ channel.

^c $1\text{-C}_4\text{H}_9$ channel.

^d $2\text{-C}_4\text{H}_9$ channel.

^e $i\text{-C}_4\text{H}_9$ channel.

^f $t\text{-C}_4\text{H}_9$ channel.

and recently, we investigated H abstraction reactions from ethane by HO_2 , CH_3O_2 and $\text{C}_2\text{H}_5\text{O}_2$ [8]. We found that the activation energies follow an Evans–Polanyi relationship and that a pre-exponential factor (given per H atom), derived from the reference reaction $\text{HO}_2 + \text{H}_2\text{O}$, provided a good description of the data. Based on the limited number of reactions considered we concluded that the empirical rate rule should also be suitable for larger alkanes and peroxy species.

The objective of the current study is to expand the earlier work and to provide a more detailed and comprehensive database of the reaction of $\text{R}'\text{O}_2$ radicals with alkanes. The main focus is on systematic trends with an eye on possibilities to generalize the results in terms of rate estimation rules suitable for, e.g., automated reaction generation software. To do so we calculated rate constants for a set of 32 reactions, which are given in Tables 1 and 2. The set includes reactions of the alkanes $\text{RH} = \text{CH}_4$, C_2H_6 , C_3H_8 , $n\text{-C}_4\text{H}_{10}$, and $i\text{-C}_4\text{H}_{10}$ with the peroxy species $\text{R}'\text{O}_2$; $\text{R}' = \text{H}$, CH_3 , C_2H_5 , $n\text{-C}_3\text{H}_7$, $i\text{-C}_3\text{H}_7$, $n\text{-C}_4\text{H}_9$, $t\text{-C}_4\text{H}_9$, $\text{HC}=\text{O}$, and $\text{CH}_3\text{C}=\text{O}$. The reactions

were selected based on the following criteria: (1) computational limitations restricted the calculations to systems containing not more than seven non-hydrogen atoms. Consequently, small $\text{R}'\text{O}_2$ species such as HO_2 and CH_3O_2 allow the largest variation in RH and, vice versa, a study of the impact of the R' moiety is only possible with small alkanes. (2) Inclusion of HO_2 as reactant enables comparisons to experimental data found in the literature. (3) Acyl peroxy species were included to expand the range of reaction enthalpies and because they are thought to be of importance in the low temperature oxidation chemistry [18]. (4) Unsaturated hydrocarbons were not considered because their kinetic behavior is more complicated since addition reactions to double bonds are now possible. This increased complexity is outside of the scope of this work, but would be an interesting topic for a future study.

The paper is structured as follows. First we give a brief description of the calculation methods used. Then the calculated rate constants are presented in terms of systematic series either with a common alkane or peroxy species. In the discus-

Table 2
Modified Arrhenius rate expressions for $\text{R}'\text{O}_2 + \text{R-H} \rightarrow \text{R}'\text{OOH} + \text{R}\cdot$ obtained from fits of TST calculations between 300–2000 K

$\text{R}'\text{O}_2$ with $\text{R}' =$	$\text{R-H} \rightarrow \text{R}\cdot$	A	n	E_a	
H	$\text{CH}_4 \rightarrow \text{CH}_3$	1.18E2	3.52	20.1	
	$\text{C}_2\text{H}_6 \rightarrow \text{C}_2\text{H}_5$	5.22E3	3.29	16.0	
	$\text{C}_3\text{H}_8 \rightarrow n\text{-C}_3\text{H}_7$	2.54E2	3.33	15.6	
	$\text{C}_3\text{H}_8 \rightarrow i\text{-C}_3\text{H}_7$	8.46E2	3.10	12.7	
	$n\text{-C}_4\text{H}_{10} \rightarrow 1\text{-C}_4\text{H}_9$	3.71E2	3.28	15.5	
	$n\text{-C}_4\text{H}_{10} \rightarrow 2\text{-C}_4\text{H}_9$	3.88E2	3.34	12.3	
	$i\text{-C}_4\text{H}_{10} \rightarrow i\text{-C}_4\text{H}_9$	2.84E3	3.36	15.8	
	$i\text{-C}_4\text{H}_{10} \rightarrow t\text{-C}_4\text{H}_9$	8.23E2	3.01	10.0	
	CH ₃	$\text{CH}_4 \rightarrow \text{CH}_3$	1.21E1	3.75	21.2
		$\text{C}_2\text{H}_6 \rightarrow \text{C}_2\text{H}_5$	4.04E1	3.55	16.9
$\text{C}_3\text{H}_8 \rightarrow n\text{-C}_3\text{H}_7$		6.71E0	3.72	16.9	
$\text{C}_3\text{H}_8 \rightarrow i\text{-C}_3\text{H}_7$		8.14E1	3.37	13.8	
$n\text{-C}_4\text{H}_{10} \rightarrow 1\text{-C}_4\text{H}_9$		1.44E1	3.70	16.8	
$n\text{-C}_4\text{H}_{10} \rightarrow 2\text{-C}_4\text{H}_9$		1.05E2	3.49	13.4	
$i\text{-C}_4\text{H}_{10} \rightarrow i\text{-C}_4\text{H}_9$		6.62E0	3.75	16.9	
$i\text{-C}_4\text{H}_{10} \rightarrow t\text{-C}_4\text{H}_9$		2.62E2	3.12	11.1	
C ₂ H ₅		$\text{CH}_4 \rightarrow \text{CH}_3$	1.24E1	3.69	21.3
		$\text{C}_2\text{H}_6 \rightarrow \text{C}_2\text{H}_5$	5.88E1	3.49	17.1
	$\text{C}_3\text{H}_8 \rightarrow n\text{-C}_3\text{H}_7$	7.14E0	3.65	17.1	
	$\text{C}_3\text{H}_8 \rightarrow i\text{-C}_3\text{H}_7$	4.02E1	3.41	14.1	
	$n\text{-C}_3\text{H}_7$	$\text{CH}_4 \rightarrow \text{CH}_3$	0.70E0	3.95	21.4
$\text{C}_2\text{H}_6 \rightarrow \text{C}_2\text{H}_5$		2.70E0	3.81	17.2	
$i\text{-C}_3\text{H}_7$		$\text{CH}_4 \rightarrow \text{CH}_3$	3.06E0	3.87	21.8
	$\text{C}_2\text{H}_6 \rightarrow \text{C}_2\text{H}_5$	1.06E1	3.69	17.5	
$n\text{-C}_4\text{H}_9$	$\text{CH}_4 \rightarrow \text{CH}_3$	2.38E0	3.87	21.6	
	$\text{C}_2\text{H}_6 \rightarrow \text{C}_2\text{H}_5$	0.96E0	3.98	21.8	
$t\text{-C}_4\text{H}_9$	$\text{CH}_4 \rightarrow \text{CH}_3$	3.22E3	3.13	15.2	
	$\text{C}_2\text{H}_6 \rightarrow \text{C}_2\text{H}_5$	4.23E3	2.96	10.5	
HC(O)	$\text{C}_3\text{H}_8 \rightarrow n\text{-C}_3\text{H}_7$	7.66E2	3.17	10.7	
	$\text{C}_3\text{H}_8 \rightarrow i\text{-C}_3\text{H}_7$	6.32E3	2.92	7.80	
	$\text{CH}_4 \rightarrow \text{CH}_3$	7.26E1	3.60	14.2	
	$\text{C}_2\text{H}_6 \rightarrow \text{C}_2\text{H}_5$	1.01E2	3.37	9.64	
CH ₃ C(O)	$\text{CH}_4 \rightarrow \text{CH}_3$	7.26E1	3.60	14.2	
	$\text{C}_2\text{H}_6 \rightarrow \text{C}_2\text{H}_5$	1.01E2	3.37	9.64	

The A factors are given in $\text{cm}^3/\text{mol}\cdot\text{s}$ and the E_a values are in kcal/mol (1 kcal/mol = 4.184 kJ/mol).

sion we will address the expected accuracy of our results and explore the possibility of formulating a rate estimation rule that would be applicable to larger hydrocarbons of interest in combustion. A short conclusion will summarize the results and address open questions.

2. Calculation methods

All required molecular properties were obtained from electronic structure calculations at the CBS-QB3 level of theory [19] as implemented in the Gaussian G98W suite of programs [20]. More specifically, geometries and frequencies were obtained with the B3LYP hybrid functional and the CBSB7 basis set. If a species exists in more than one conformation, the lowest energy conformer (at 0 K) was identified and used in the subsequent analysis. The atomization method was employed to convert the electronic energy into the corresponding heat of formation, and we calculated the entropy and heat capacity values with methods from statistical mechanics. All calculations assume that the harmonic-oscillator-rigid-rotor approximation is valid. Harmonic frequencies were scaled by a factor of 0.99 prior to their use in the calculation of zero point energies and vibrational partition functions. Large amplitude vibrational modes describing internal rotations were treated separately: first we calculated the hindrance potential via a relaxed potential energy scan in steps of 20 degrees around the rotating bond. This potential was approximated with a truncated Fourier series ($n = 5$). The corresponding averaged moment of inertia belonging to an internal rotor was approximated at the $I^{(2,3)}$ level as defined by East and Radom [21] based on the work by Kilpartick and Pitzer [22]. With this information at hand, the Schroedinger equation was solved numerically using the wave functions of the free rotor as basis function. The solution yields a set of energy eigenvalues, which were used to calculate the contribution of this mode to the thermodynamic functions H , S , and C_p . The described methodology was applied to stable species as well as to transition states.

In terms of the Gibbs free energy of reaction, ΔG^\ddagger , the bimolecular TST rate constant may be calculated via

$$k_{\text{TST}}(T) = \kappa(T) \cdot k_B T / h \cdot V_{\text{mol}} \cdot \exp(-\Delta G^\ddagger / RT).$$

V_{mol} is the molar volume and ΔG^\ddagger is the difference of the Gibbs free energies of the transition state (excluding the transitional mode) and the reactants. The temperature dependent transmission factor $\kappa(T)$ accounts for contributions from tunneling. We used Wigner's method [23]

$$\kappa(T) = 1 + 1/24.0 \cdot (1.44 \cdot v_{\text{im}}/T)^2,$$

which only requires the imaginary frequency of the transition state as input parameter. Since the imaginary frequencies are very similar for all reactions studied, the tunneling corrections have no pronounced impact on the observed relative reactivities. At 300 K the correction hardly exceeds a factor of four and at temperatures relevant to autoignition it is well below a factor of two. We previously [8] compared transmission factors obtained with Wigner's method to those derived from asymmetric Eckart potentials [24] and found that both methods yield very similar results for this type of reaction.

3. Results

The objective of this study is to better characterize the kinetics of $R'O_2$ abstraction reactions with alkanes. To do so we calculated rate constants for a total of 32 reactions involving five different alkanes and nine different peroxy radicals. Particular aspects of the results are graphically presented in Figs. 1 and 2. In addition we report rate constants for all reactions at 600 K and 800 K in Table 1, and the modified Arrhenius expressions in Table 2. The choice to provide multiple presentations of the same results is guided by the goal to clearly describe the general features.

The first focus will be on the abstraction from methane, because we could investigate the largest range of peroxy species within our computational limitations. Results for nine reactions are plotted in Fig. 1a. Three groups of rate constants can obviously be distinguished. The reaction rate constants for all alkyl peroxy radicals ($R' = \text{CH}_3$, C_2H_5 , $n\text{-C}_3\text{H}_7$, $i\text{-C}_3\text{H}_7$, $n\text{-C}_4\text{H}_9$, and $t\text{-C}_4\text{H}_9$) are rather similar and form a comparatively narrow band in the plot. The rate constant for HO_2 as the abstracting species is larger and clearly separated. Finally, the acyl peroxy radicals HC(O)O_2 and $\text{CH}_3\text{C(O)O}_2$ react fastest, by more than three orders of magnitude at room temperature compared to HO_2 . An assessment of the reactivity differences at temperatures relevant to ignition is possible from the entries in Table 1. The acyl peroxy radicals react with CH_4 one to two orders of magnitudes faster than HO_2 , which in turn is distinguishably more reactive, even at 800 K, than alkyl peroxy species. In general, all rate constants increase substantially between 600 and 800 K but the increase is most pronounced for the alkyl peroxy radicals. A final note on the data given for CH_4 in Table 1: within the group of alkyl peroxy species, it appears as if the reaction rate constant decreases slightly with increasing molecule size, however, the entry for n -propyl peroxy does not fit into this trend (we will comment on this later). The observations just described for methane also hold for the abstraction from ethane. This is

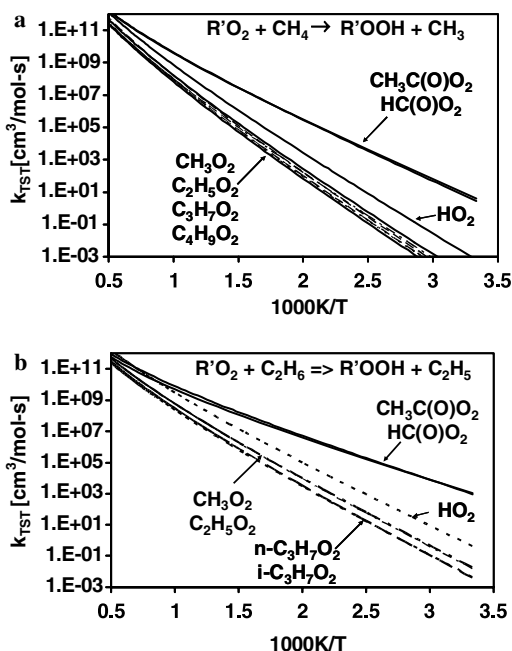


Fig. 1. Rate constants for the H atom abstraction from (a) CH_4 and (b) C_2H_6 by $\text{R}'\text{O}_2$ radicals.

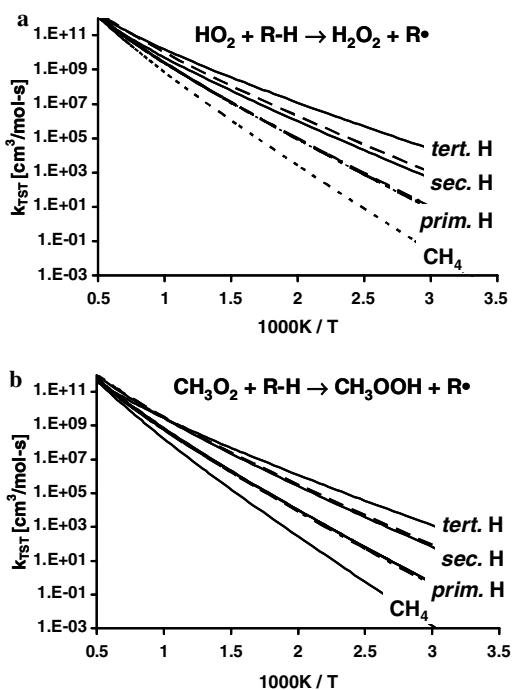


Fig. 2. Rate constants for the H atom abstraction by (a) HO_2 and (b) CH_3O_2 from alkanes (R-H).

shown in Fig. 1b. Here the reactivity trends within the group of alkyl peroxy radicals are more distinguishable than for methane. Note that the rate constants for methyl peroxy and ethyl peroxy are virtually identical. This is in agreement with our previous work, though the data presented here are from new and independent calculations. Replacing *n*-propyl peroxy with *i*-propyl peroxy does not significantly change the reactivity.

Next, we address the influence of the nature of the alkane on the reactivity of a given peroxy species. Results are shown in Fig. 2a for HO_2 and in Fig. 2b for CH_3O_2 (results for $\text{C}_2\text{H}_5\text{O}_2$ are similar to CH_3O_2). As expected, the reactivity is strongly related to the strength of the C–H bond that is attacked. Consequently CH_4 is the least reactive alkane, followed by abstraction reactions involving a primary C–H (e.g., formation of C_2H_5 , *n*- C_3H_7 , *n*- C_4H_9 , and *i*- C_4H_9), then secondary C–H bonds (leading to *i*- C_3H_7 , *sec*- C_4H_9), and finally the reaction to form *tert*-butyl is fastest. Notably all calculated rate constants for primary C–H abstractions by HO_2 are almost identical even though *iso*-butane contains nine equivalent H atoms and should be faster by a factor of 3/2 based on statistical arguments. While this statistical factor is not apparent in the calculations for primary C–H bonds, it is qualitatively resolved for the reactions of secondary C–H bonds. The dashed line in Fig. 2a corresponding to the rate constant for *n*-butane reacting to *n*-but-2-yl is clearly above the solid line for the formation of isopropyl and a look into Table 1 confirms that the rate constants differs at both temperatures by about a factor of 1.5–2. The expected difference is even more clearly seen in the case of CH_3O_2 , but this might be coincidence because now the rate constants for primary C–H abstraction deviate more.

The major conclusion from the results is that the H abstraction reactivity of all peroxy radicals is dominated by the activation energy. This is supported by the modified Arrhenius rate parameters given in Table 2. The fitted activation energies correlate well with the C–H bond type and also with the trends seen for the different $\text{R}'\text{O}_2$ species. In addition, the temperature exponents for all reactions are large and positive, indicating strong non-Arrhenius behavior as one would expect for this type of reaction. The fitted values for *n* over 300–2000 K are around 3.5 with extremes of about 2.9 and 4.0. However, since alkyl peroxy radicals decompose at elevated temperatures, these reactions will not be important beyond 1000 K.

4. Discussion

All rate constants presented are based on theoretical calculations. Hence it seems prudent to first address the reliability of these results prior to

attempting to generalize them so they can be used in oxidation mechanisms of larger hydrocarbons. As pointed out in the Section 1, experimental data are only available for HO_2 . In Fig. 3, we compare rate constants for CH_4 , C_2H_6 , C_3H_8 , and $i\text{-C}_4\text{H}_{10}$ as reported by Scott and Walker [13] to our predictions. We recognize two important facts: (1) the calculated values are systematically above the experimental data and (2) the slopes in the Arrhenius plots agree very well. For clarity reasons we did not indicate error margins for the measurements, but those given by Scott and Walker [13] for the pre-exponential factor are actually large enough to include our calculated values. Further taking into account that the experimental values are extracted from relative measurements (related to HO_2 recombination) it seems that the agreement is reasonable. On the other hand, one might interpret these comparisons to mean that they suggest a systematic error in the calculated pre-exponential factors. This raises the general question regarding the expected accuracy of the calculations.

One area of uncertainty originates from treating all vibrations as harmonic. If some modes experienced severe anharmonic behavior, the harmonic-oscillator-rigid-rotor assumption would break down. However, as long as similar anharmonic effects occur in the reactants and transition state, they would cancel when calculating the TST rate constant. On the other hand, if anharmonic oscillations involve atoms that participate in the reaction, these might not be conserved and hence could have a noticeable impact on the results. Peroxy radicals are known for their weak $\text{R}'\text{-O}_2$ bonds, which lead to an anharmonic stretch vibration. Since this bond is considerably stronger in the $\text{R}'\text{OOH}$ product, one would expect it to be strengthened in the transition state as well. Simultaneously, the O-O bond, which is strong in the peroxy radicals, weakens. Taking alkyl peroxy radicals as an example, the $\text{R}'\text{-O}_2$ bond is around

35 kcal/mol but the O-O bond energy is almost 10 kcal/mol higher. Consequently, it is conceivable that anharmonicity effects might have a larger impact on the reactants (peroxy species) than on the transition states. Since Morse type oscillations lead to larger partition functions (and entropies), this would suggest that neglecting this effect could tend to over-predict the rate constants. However, it should be noted that looking at an isolated vibration is a over-simplification since anharmonicity also affects the rotational partition functions and other vibrational modes via coupling.

A related problem is the existence of a low-lying electronically excited state, which is thought to be involved in the unimolecular dissociation of $\text{R}'\text{O}_2$ radicals [25]. Mixing of excited state with ground state levels could increase the density of states in the reactants and reduce again the rate constants. This idea is supported by results from the ethyl + O_2 reaction that point to a larger than expected collision stabilization rate constant for $\text{C}_2\text{H}_5\text{O}_2$ [7].

Another source of error relates to the selection of low frequency modes that resemble hindered rotations. We assign these frequencies by inspecting animated vibrations, but in some cases the assignment proves very ambiguous. Interestingly we find that calculated rate constants that fall outside of a general trend (e.g., that for the reaction $n\text{-C}_3\text{H}_7\text{O}_2 + \text{CH}_4$) correlate with such assignment problems. A possible cause could be that some geometry optimizations were not precise enough and that frequency calculations based on these are inaccurate. This could also explain the observation that conformers of transition state structures for large reactants differ considerably in their frequency spectra although they are very similar in energy. We plan to investigate this issue in the future.

In summary, even though electronic structure calculations can yield accurate energies, considerable uncertainties regarding the calculation of entropy values remain. This is particularly true for floppy species such as larger transition states. In our previous work concerning abstraction from ethane, we estimated the uncertainty of the pre-exponential constant to be about a factor of two [8]. The uncertainty is possibly twice as large for some reactions considered in this study. Given these estimates, one could be inclined to ignore the spread of rate constants observed for the alkyl peroxy reactions with methane and ethane (Fig. 1) and to consider just the averaged value. But this could be an over-simplification because the rate constant declines (except for one case) systematically with increasing molecular size. Therefore structural effects cannot be ruled out.

To support the correlation between calculated activation energies and the heat of reaction, we show in Fig. 4 Evans–Polanyi type plots for the

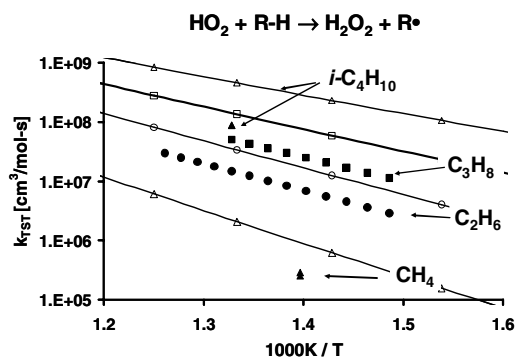


Fig. 3. Comparison of calculated and experimental rate constants for H atom abstraction by HO_2 . Closed symbols: experimental data from Scott and Walker [13]; lines and open symbols: calculated values.

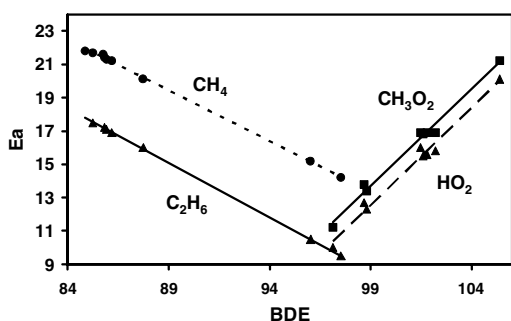


Fig. 4. Evans–Polanyi plots (activation energy versus the bond dissociation energy of the appropriate hydrogen bond, both in kcal/mol) for four reaction sets: $R'O_2 + CH_4$, $R'O_2 + C_2H_6$, $HO_2 + RH$, $CH_3O_2 + RH$.

same four reaction series that are plotted in Figs. 1 and 2. More specifically, we plot the activation energies from the modified Arrhenius fits versus the bond dissociation energy (BDE) of the attacked hydrogen bond or of the formed O–H bond, respectively. The linear relationships are clearly observable despite some scatter in the alkane series. Noting that the temperature exponent, which was not held constant, affects the value of the activation energy, this scatter is not surprising. The following four relationships were obtained from the plots (in kcal/mol):

$$CH_4 \text{ series: } E_a = 73.6 - 0.61 \cdot BDE(R'OO-H)$$

$$C_2H_6 \text{ series: } E_a = 73.3 - 0.65 \cdot BDE(R'OO-H)$$

$$HO_2 \text{ series: } E_a = -103.1 + 1.17 \cdot BDE(R-H)$$

$$CH_3O_2 \text{ series: } E_a = -101.6 + 1.17 \cdot BDE(R-H)$$

The slope of the straight line fit for C_2H_6 of 0.65 might be compared with the value of 0.60 we proposed in the former study [8]. Since one would normally expect the slope of Evans–Polanyi plots to be within the range of 0–1, the values for the $R'O_2$ sets are somewhat surprising. Perhaps they can be explained with polarization effects that lead to an additional stabilization of the transition states. A Mulliken population analysis for the transition states should allow clarification of this point.

The activation energies of the entire set of 32 reactions can be approximated by a combined Evans–Polanyi type relationship containing the bond dissociation energies of both, the hydroperoxide and the alkane as independent variables:

$$E_a = -46.8 - 0.616 \cdot BDE(R'OO-H) + 1.149 \cdot BDE(R-H) \quad [\text{in kcal/mol}]$$

We found an average deviation of about 0.1 kcal/mol and a maximum error of 0.5 kcal/mol.

Inspection of the fitted activation energies revealed that the errors are not statistically distributed among the alkanes. Instead all seven reactions for which we observed a deviation of more than 0.15 kcal/mol between calculated and predicted activation energies involve either propane or a butane isomer as reactant. This clearly indicates a size effect—at least according to our calculations.

We also tried to identify a common pre-exponential factor—on a per hydrogen basis—that can reproduce all rate constants, but this attempt failed. Even for the subset of alkyl peroxy abstractions such a single pre-exponential factor does not represent the rate constants. Contrary to our expectations, this study reveals that structural changes have an impact on the pre-exponential factors that goes beyond a change of the number of available hydrogens. Though the activation energy is the dominant controlling parameter for this class of reactions, structural properties appear to be important as well.

Finally, we would like to address the implications of this study. The calculations were motivated by a search for additional chain-branching in the low temperature oxidation of hydrocarbons. In order to contribute to the production of radicals, the abstraction reaction has to fulfill two requirements: (1) it has to be fast enough to compete with other $R'O_2$ consumption paths and (2) the resulting $R'OOH$ molecule should have a O–O bond weak enough to allow decomposition at low temperatures (e.g., the NTC region). The O–O bond energy in alkyl hydroperoxides of about 44 kcal/mol is weak and decomposition is sufficiently fast. However, the abstraction rate constants are the smallest among the peroxy reactions studied. In the case of ethane oxidation our calculations showed an observable impact on ignition times [8], but, since larger alkyl peroxy radicals have alternative lower energy isomerization pathways, the H atom abstraction reaction from the parent is most likely not longer competitive. On the other hand, most olefins produced via the concerted elimination reaction of large alkyl peroxy radicals contain reactive allylic hydrogens. In addition, substantial concentrations of aldehydes with reactive C–H bonds are produced during low temperature ignition. This opens the possibility that $R'O_2$ abstraction from alkenes and aldehydes could yield $R'OOH$ and future studies should address these reactions.

A different situation exists for the abstraction reactions by HO_2 . H_2O_2 production from H abstraction is faster but the stronger HO–OH bond makes it too stable to contribute to autoignition at low temperatures. In addition it should be noted that more efficient H_2O_2 product channels exist, which make it unlikely that the abstraction reactions considered in this study will have a noticeable impact.

Finally, the calculated large rate constants for H abstraction by acyl peroxy radicals make it conceivable that these reactions play a role in oxygen rich low temperatures ignition systems as has been proposed by Dechaux and Delfosse [18]. Preliminary results from electronic structure calculations at the CBS-QB3 level of theory yielded a bond dissociation energy of about 47 kcal/mol for $\text{CH}_3\text{C}(=\text{O})\text{OOH}$, which is about 3 kcal/mol lower than the value for H_2O_2 . (For $\text{HC}(=\text{O})\text{OOH}$ we found a significantly higher value of 53 kcal/mol.) Assuming a low value for $\text{RC}(=\text{O})\text{OOH}$ can be confirmed, this opens the possibility that the thermal decomposition of peracids formed via the reactions discussed in this paper could provide additional chain-branching. Further investigations are needed to clarify this possibility.

5. Conclusion

We presented transition state calculations of rate constants for a total of 32 hydrogen abstraction reactions involving alkanes up to C_4 and nine different peroxy species. The reactivity order (acyl peroxy $>$ HO_2 $>$ alkyl peroxy) is mainly determined by the strength of the formed O–H bond and it is possible to represent the activation energies with reasonable accuracy with a single relationship containing the bond dissociation energies of both $\text{R}'\text{OOH}$ and R–H as variables. A single expression for the pre-exponential factor, however, could not be found. This suggests that structural properties of the alkyl peroxy radical and of the alkane cannot be neglected. A consequence of this increased complexity is that the simple estimation rule we hoped to develop has proven elusive. More conclusive calculations addressing the steric effect would require improvements in the calculation of entropies of floppy molecules.

References

[1] R.W. Walker, C. Morley, in: M.J. Pilling (Ed.), *Low-Temperature Combustion and Autoignition*, Elsevier, Amsterdam, 1997, pp. 1–124.

Comments

John Simmie, National University of Ireland, Ireland.
Why did you use an atomization method in CBS-QB3 computations as against the normally better regarded isodesmic procedure?

Reply. Electronic structure calculations yield as primary output electronic energies which have to be converted to heats of formation if thermodynamic

- [2] J.W. Bozzelli, C. Sheng, *J. Phys. Chem. A* 106 (2002) 1113–1121.
 [3] E.W. Kaiser, *J. Phys. Chem. A* 106 (2002) 1256–1265.
 [4] J.C. Rienstra-Kiracofe, W.D. Allen, H.F. Schaefer III, *J. Phys. Chem. A* 104 (2000) 9823–9840.
 [5] J.A. Miller, S.J. Klippenstein, *Int. J. Chem. Kinet.* 33 (2001) 654–668.
 [6] C.Y. Sheng, J.W. Bozzelli, A.M. Dean, A.Y. Chang, *J. Phys. Chem. A* 106 (2002) 7276–7293.
 [7] H.-H. Carstensen, C.V. Naik, A.M. Dean, *J. Phys. Chem. A* 109 (2005) 2264–2281.
 [8] H.-H. Carstensen, A.M. Dean, *Proc. Combust. Inst.* 30 (2005) 995–1003.
 [9] R.R. Baldwin, P.N. Jones, R.W. Walker, *J. Chem. Soc. Faraday Trans. 2* 84 (1988) 199–207.
 [10] R.R. Baldwin, C.E. Dean, M.R. Honeyman, R.W. Walker, *J. Chem. Soc. Faraday Trans. 1* 82 (1986) 89–102.
 [11] S.M. Handford-Styring, R.W. Walker, *Phys. Chem. Chem. Phys.* 3 (2001) 2043–2052.
 [12] S.M. Handford-Styring, R.W. Walker, *Phys. Chem. Chem. Phys.* 4 (2002) 620–627.
 [13] M. Scott, R.W. Walker, *Combust. Flame* 129 (2002) 365–377.
 [14] R.R. Baldwin, M.W.M. Hisham, R.W. Walker, *J. Chem. Soc. Faraday Trans. 1* 78 (1982) 1615–1627.
 [15] W. Tsang, R.F. Hampson, *J. Phys. Chem. Ref. Data* 15 (1986) 1087–1279.
 [16] W. Tsang, *J. Phys. Chem. Ref. Data* 17 (1988) 887–951.
 [17] W. Tsang, *J. Phys. Chem. Ref. Data* 19 (1990) 1–68.
 [18] J.C. Dechaux, L. Delfosse, *Combust. Flame* 34 (1979) 169–185.
 [19] J.A. Montgomery Jr., M.J. Frisch, J.W. Ochterski, G.A. Petersson, *J. Chem. Phys.* 110 (1999) 2822–2827.
 [20] M.J. Frisch, G.W. Trucks, H.B. Schlegel, et al., Gaussian 98, Revision A.11, Gaussian, Inc., Pittsburgh, PA (1998).
 [21] A.L.L. East, L. Radom, *J. Chem. Phys.* 106 (1997) 6655–6674.
 [22] J.E. Kilpatrick, K.S. Pitzer, *J. Chem. Phys.* 17 (1949) 1064–1075.
 [23] E. Wigner, *Z. Phys. Chem. B* 19 (1932) 203–216.
 [24] C. Eckart, *Phys. Rev.* 35 (1930) 1303–1309.
 [25] A. Andersen, E.A. Carter, *J. Phys. Chem. A* 106 (2002) 9672–9685.

properties are needed. Both, the atomization method as well as the formulation of isodesmic reaction systems can be employed for this task.

We prefer the method of atomization for several reasons. First, the CBS-QB3 and other compound methods were developed based on atomization energies. Second, the methodology is uniquely defined and easily implemented into software. Third, it can

also be used for unusual species for which no reference molecules are available to work with isodesmic reactions. And last, it works for transition states as well. The strength of isodesmic reactions, which is cancellation of systematic bond errors, can be incorporated into the atomization scheme by employing bond additivity corrections. One should note that for the purpose of this study neither method is necessarily needed, since TST calculations in principle require only relative energies. Only because we chose to use the ΔG formalism we converted the electronic energies to heats of formation.

•

S. Dóbe, Chemical Research Center, Budapest, Hungary. My question is concerned with the reaction $\text{HO}_2 + \text{CH}_3\text{CHO}$ which may have relevance to atmo-

spheric chemistry as well. Did you see an indication for the occurrence of addition of HO_2 to the carbonyl CdbondO bond?

Reply. This study focuses exclusively on abstraction reactions from alkanes to avoid complications such as the occurrence of addition pathways mentioned in the question. With respect to $\text{HO}_2 + \text{CH}_3\text{CHO}$, it is well known that an addition complex of the structure $\text{CH}_3\text{CH}(\text{OH})\text{O}_2$ can be formed via H atom migration to the carbonyl oxygen following the addition step. This complex is according to preliminary CBS-QB3 calculations approximately 10–15 kcal/mol more stable than the reactants. A complete kinetic analysis of this and similar systems has not yet been done due to the increased complexity resulting from H bonding, identification and characterization of product channels, and treatment of pressure-dependence. We plan to address this type of reaction in the future.